

The synergy reduction and self-assembly of graphene oxide via gamma-ray irradiation in an ethanediamine aqueous solution

Ya-Lei He^{1,2} · Ji-Hao Li² · Lin-Fan Li² · Jing-Bo Chen¹ · Jing-Ye Li²

Received: 25 January 2016/Revised: 29 February 2016/Accepted: 13 March 2016/Published online: 11 May 2016
© Shanghai Institute of Applied Physics, Chinese Academy of Sciences, Chinese Nuclear Society, Science Press China and Springer Science+Business Media Singapore 2016

Abstract Gamma-ray irradiation technique is an effective method for preparing graphene aerogel (GA). The effective reduction and self-assembly of graphene oxide (GO) sheets into 3D porous GA in ethylenediamine (EDA) aqueous solution under the protection of nitrogen have been achieved via γ -ray irradiation. The reduction degree and self-assembly process, which can be controlled by varying EDA dose and irradiation dose, are investigated by X-ray photoelectron spectroscopy, Fourier transform infrared spectroscopy, X-ray diffractometer, and thermogravimetric analysis. A reduction mechanism is proposed for interactions among EDA molecules, active radicals from the radiolysis of water, and oxygen-containing groups on GO sheets.

Keywords Gamma-ray irradiation · Reduction and self-assembly · Graphene oxide · Graphene aerogel · Ethanediamine

1 Introduction

Gamma-ray irradiation, a low-cost, maneuverable, and environment-friendly method for synthesis, modification, and processing of polymeric materials [1], has been widely used in preparation of metallic nanoparticles [2], modification of polymers [3], and disposal of pollutants [4]. ⁶⁰Co γ -rays can induce chemical reactions uniformly, without catalyst, at any temperature and any phase, facilitating industrialization [5].

According to the radiation chemistry of water, the as-formed strong reductive agents like aqueous electron (e_{aq}^-) and hydrogen radicals (H \cdot) [6] during γ -ray irradiation process can be utilized for in situ preparation of nanoparticles in aqueous solution by reducing their precursors. There are reports about the reduction and/or modification of graphene oxide (GO) via γ -ray irradiation in different solvents, including alcohol/water and *N,N*-dimethyl formamide [7, 8], or even gases like hydrogen [9].

Integration of graphene oxide, reduced graphene oxide (rGO), and their derivatives into macroscopic structures has emerged as one of the most appealing strategies to develop unprecedented graphene-based functional materials. Graphene aerogel (GA), owing to its highly porous structure and large accessible surface area, has received tremendous attention in many fields such as energy conversion and storage [10], sensors [11], catalysts [12], and environmental remediation [13, 14].

On the basis of our previous study, GO sheets were successfully reduced and modified by γ -ray irradiation in an EDA/water blend solution under N₂ protection [15]. We found that the EDA played a role as a radical scavenger like alcohols during the irradiation reduction reaction. Therefore, it is reasonable that using concentrated GO

Ya-Lei He and Ji-Hao Li contributed equally to this work.

✉ Jing-Bo Chen
jingyeli@sinap.ac.cn

✉ Jing-Ye Li
chenjb@zzu.edu.cn

¹ School of Materials Science and Engineering, Zhengzhou University, Zhengzhou 450002, China

² CAS Center for Excellence on TMSR Energy System, Shanghai Institute of Applied Physics, Chinese Academy of Sciences, Shanghai 201800, China

sheets and higher total absorbed dose, we shall obtain graphene aerogel after freeze-drying the hydrogel.

In this paper, we study the reduction degree and self-assembly process through varying EDA dose and the total absorbed dose for preparing graphene aerogel. Possible reduction reaction mechanism is proposed for interactions among EDA molecules, active radicals from the radiolysis of water, and oxygen-containing groups of GO sheets.

2 Experimental

2.1 Materials

Natural graphite flakes ($\sim 500\ \mu\text{m}$) were purchased from Sigma-Aldrich to synthesize graphene oxide. Concentrated sulfuric acid (H_2SO_4 , 98 %), concentrated nitric acid (HNO_3), potassium persulfate ($\text{K}_2\text{S}_2\text{O}_8$), phosphorus pentoxide (P_2O_5), potassium permanganate (KMnO_4), hydrogen peroxide (H_2O_2 , 30 %) solution, hydrochloric acid (HCl), ethylenediamine (EDA), ethanol were purchased from Sinopharm Chemical Reagent Co., Ltd., China. Ultrapure water (Milli-Q purification system, Millipore, USA) was used for all experiments.

2.2 Preparation of GA

GO was prepared from natural graphite flakes on the basis of a modified Hummers' method as mentioned in previous work [14]. The GO sheets are about $20\ \mu\text{m}$ thick. In a typical procedure of GA synthesis, 10 mL homogeneous mixture of GO and EDA aqueous suspension (in GO/EDA weight ratio of 1:0, 1:5, 1:10, 1:20, and 1:50) was filled into a glass vial, deoxygenated by N_2 bubbling for 10 min, and sealed for irradiation to 100–500 kGy at a dose rate of 4.55 kGy/h in a ^{60}Co cell at room temperature. After irradiation, the non-reacted EDA and extra ions were removed by alternate dialysis with HCl acid, water, and ethanol for over five cycles. Eventually, the as-prepared graphene hydrogel was subjected to freeze-drying to obtain the final graphene aerogel. The GO concentration in the final mixture was 2 mg/mL, and the irradiation dose was 200 kGy.

2.3 Characterizations

Scanning electron microscope (SEM) images were recorded on a field emission SEM (JEOL, JSM-6700F) at 10 kV.

X-ray photoelectron spectroscopy (XPS) was performed on a SHIMADZU Kratos AXIS Ultra DLD XPS instrument equipped with a monochromated Al $\text{K}\alpha$ X-ray source. High-resolution scans were acquired at 40 eV pass energy,

and wide-scan survey spectra were acquired at 160 eV pass energy.

Fourier transform infrared (FT-IR) spectra were collected using KBr pellets on the transmission module of Thermo Nicolet Avatar 370 FT-IR spectrometer at $4\ \text{cm}^{-1}$ resolution and 32 scans.

X-ray diffraction (XRD) patterns were collected on a Rigaku D/Max 2200 X-ray diffractometer with $\text{Cu-K}\alpha$ ray ($\lambda = 1.54\ \text{\AA}$) at 40 kV and 50 mA. All experiments were carried out in the reflection mode at ambient temperature with $2\theta = 5^\circ\text{--}50^\circ$. The scanning speed was set at $8^\circ\ \text{min}^{-1}$.

Thermal gravity analysis (TGA) curves were recorded on a NETZSCH TG 209 F3 Tarus-Thermo-Microbalance. The samples were heated from 50 to $650\ ^\circ\text{C}$ at $10\ ^\circ\text{C}\ \text{min}^{-1}$ under $20\ \text{mL}\ \text{min}^{-1}$ of nitrogen purging. All tests were maintained at $100\ ^\circ\text{C}$ for 5 min to eliminate the influence of absorbed water.

3 Results and discussion

The whole process of γ -ray irradiation-induced self-assembly of GO sheets with different GO/EDA weight ratios and varying total absorbed dose is demonstrated in Fig. 1a and b. Figure 1a shows the sample without EDA (GO:EDA = 1:0, as a control group). Although the GO aqueous solution became thicker after 200-kGy irradiation, rGO hydrogel could not be obtained. Figure 1b shows the sample of GO/EDA = 1:10, rGO hydrogel could not be obtained at 100 kGy, either. So certain amount of EDA and certain dose are necessary for the formation of rGO hydrogel. After freeze-drying, lightweight GA with metallic luster can stand on the stamens of a flower (Fig. 1).

SEM images of the as-prepared GA (Fig. 1c–e) show that their external surfaces are quite smooth and flat except for some wrinkles, and interconnected porous structure is constructed with stacked rGO sheets. The pore size of the network ranges between 8 and $15\ \mu\text{m}$. In addition, microstructures of the GA prepared under different conditions do not differ obviously from each other, confirming that the formation of well-defined porous structure tends to be affected by freeze-drying method once the self-assembly process is accomplished at the same GO concentration [16].

XPS is utilized to analyze the surface chemistry. Figure 2 shows the normalized XPS full-scan spectra of GA of different GO/EDA ratios, and analysis results of the C, N, and O in the samples are given in Table 1. From Fig. 1 and Table 1, the C/O ratio increases dramatically at first with GO/EDA ratio, while the increase rate slows down quickly when more EDA is added into the GO aqueous solution.

According to the comprehensive analysis of C1 s spectrum profile about GO (Fig. 3a) and GO:EDA = 1:0

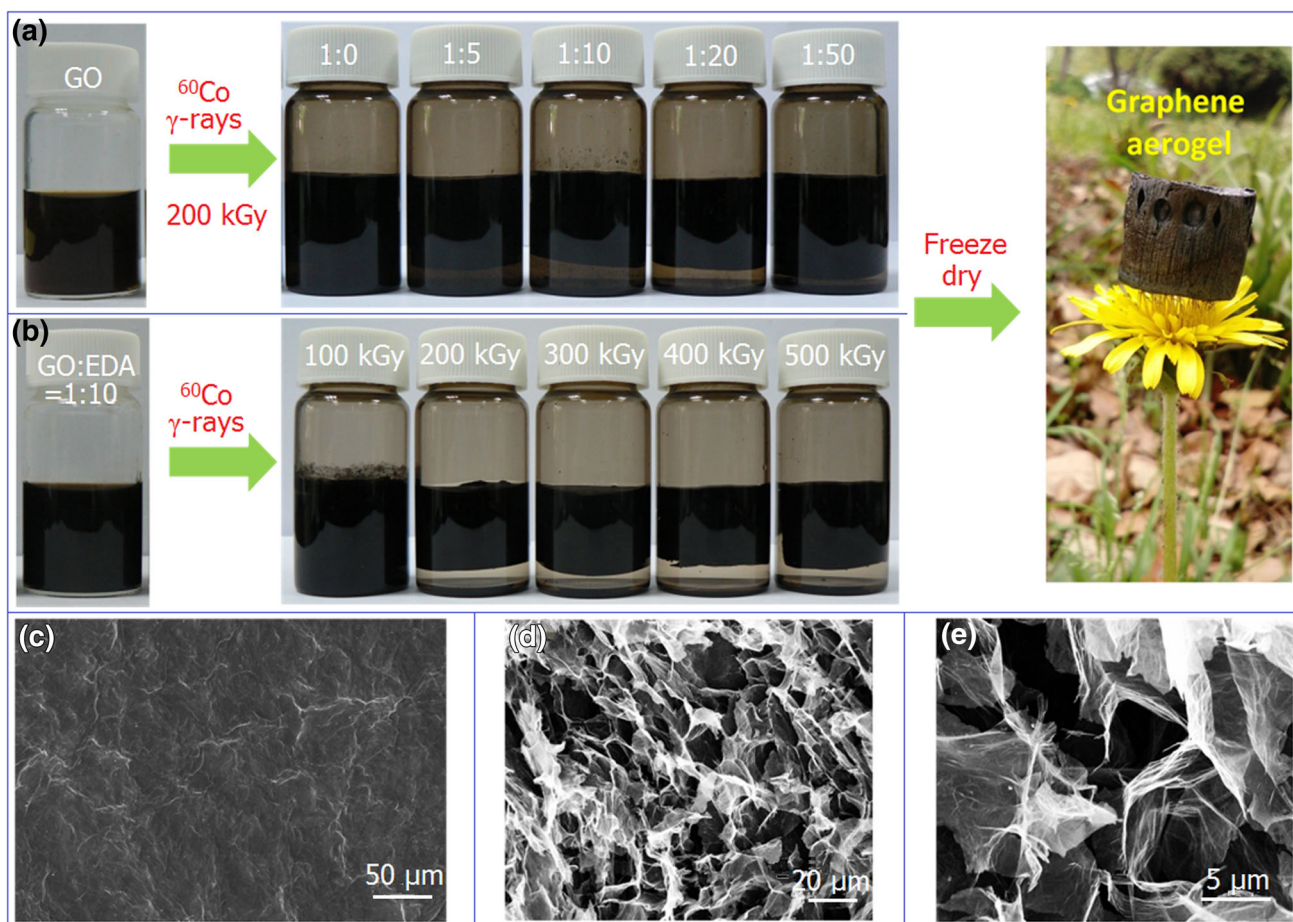


Fig. 1 Overview of the synthesis of GA under different conditions via γ -ray irradiation and freeze-drying method (a, b), SEM images of the GA surface (c) and cross section (d), and SEM image of the GA in greater magnification (e)

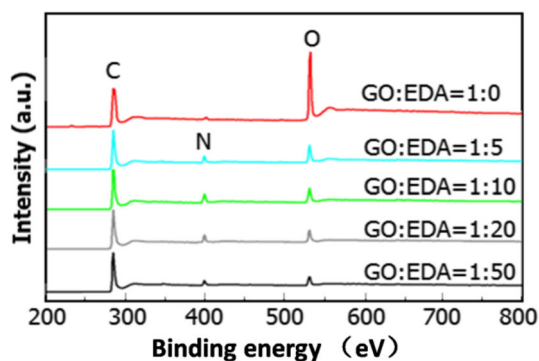


Fig. 2 XPS spectra of samples of different GO/EDA ratios

(Fig. 3b), and the analysis results in Table 2, the percent sp^3 C–C in aromatic rings, C–OH, and –COOH increases, while the percent sp^2 C–C and C–O–C decreases [17–19]. To our knowledge, epoxy groups on the basal plane of GO sheets are relatively unstable and apt to participate in ring-opening reactions under the attack of reductive radicals produced by decomposing water molecules during γ -ray

Table 1 Elemental analysis data of samples of different GO/EDA ratios

GO/EDA	Weight percentage			Elemental ratio	
	C	N	O	C/O	C/N
1:0	57.41	1.97	40.62	1.88	34.00
1:5	73.94	8.35	17.70	5.57	10.33
1:10	74.52	10.94	14.54	6.83	7.95
1:20	76.33	10.07	13.60	7.48	8.84
1:50	80.73	7.19	12.09	8.90	13.10

irradiation [14, 20]. Hydrogen radical $H\cdot$, as a powerful reductive radical, may react with the unstable C–O–C groups, which contributes to the increase in C–OH content consequently [9]. However, the reduction degree of GO aqueous solution without EDA is still very low and GO sheets could not self-assemble. In Fig. 3c–f, for all the samples with EDA component, two new peaks at 286.2 and 287.8 eV belong to C–N and NH–C=O, respectively,

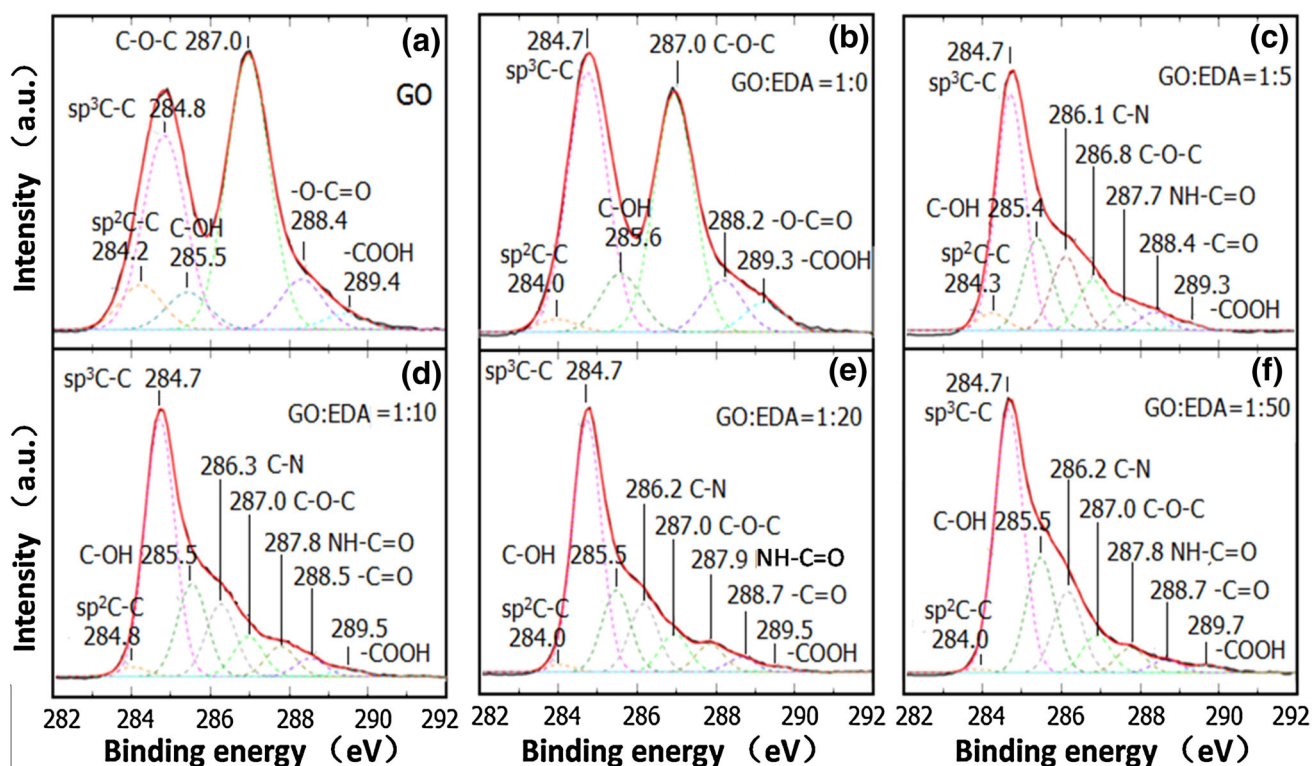


Fig. 3 C1s spectra of the samples at different GO/EDA ratios

Table 2 XPS-peak-differentiation-imitating information of samples of different GO/EDA ratios

GO/EDA	sp ² C-C	sp ³ C-C	C-OH	C-N	C-O-C	NH-C=O	-C=O	-COOH
GO	7.30	31.51	6.07	–	44.39	–	8.18	2.55
GO:EDA = 1:0	2.00	39.93	9.07	–	36.41	–	7.99	4.60
GO:EDA = 1:5	3.36	45.21	17.65	14.15	9.64	5.05	3.51	1.43
GO:EDA = 1:10	1.82	48.70	17.53	13.76	7.56	5.72	3.46	1.45
GO:EDA = 1:20	1.53	50.67	16.55	13.83	7.72	5.63	2.95	1.12
GO:EDA = 1:50	0.68	48.07	21.09	14.83	6.82	4.59	2.43	1.49

indicating the successful reactions between EDA molecules and functional groups on GO sheets under irradiation [21]. With the increase in EDA content, the percentages of all oxygen-related functional groups tend to be lower, while the percentage of C–OH remains almost the same even the weight ratio of GO/EDA reaches to 1:50.

FT-IR measurements of the samples also demonstrate the evolution of oxygen-containing groups at different GO/EDA ratios. As shown in Fig. 4a, the characteristic peaks of GO appear at 1720, 1620, 1403, 1229, and 1055 cm⁻¹ corresponding to C=O stretching vibrations from carbonyl and carboxyl groups, aromatic C–C stretching or skeletal vibrations of graphitic domains, O–H bending vibrations from hydroxyl groups, C–O stretching vibration from epoxy, and alkoxy, respectively [22, 23]. For GO aqueous solution treated with γ -ray irradiation, there is not any dramatic decrease in oxygen-containing groups except for

the shifting of some characteristic peaks. For the samples with EDA serving as additive, the characteristic peaks about oxygen-containing groups at 1055, 1229, and 1403 cm⁻¹ decrease significantly, and the characteristic peak of C=O at 1720 cm⁻¹ even disappears totally. Furthermore, some new peaks appear at 1685, 1560, 1357, and 1175 cm⁻¹ belonging to C=O in amide group, N–H, CH₂, and C–N, respectively, which indicates the successful elimination of oxygenous groups and introduction of EDA molecules corresponding to the results of XPS [20]. Along with the increase in EDA content, the difference between samples nearly cannot be observed apart from a little peak shift.

Figure 4b shows X-ray diffraction patterns of the as-prepared GA of different GO/EDA ratios. For the irradiated GO samples, a broaden diffraction peak appears at 10.00° corresponding to a *d*-spacing of 8.34 Å, which is close to

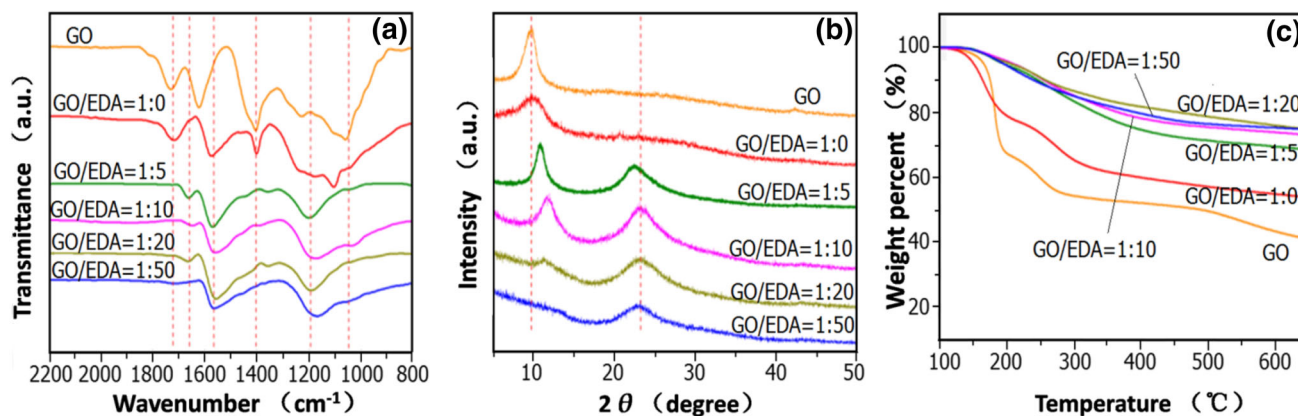


Fig. 4 FT-IR spectra (a), XRD patterns (b), and TGA curves (c) of GO and the samples at different GO/EDA ratios

the characteristic diffraction peak of GO (9.80°, d -spacing = 9.01 Å). For GA at GO/EDA = 1:5, there are both characteristic peak of GO at 11.28° and rGO at 23.25°. With increasing EDA content, the relative intensity of peak belonging to GO decreases gradually and its peak position moves to higher degree, while the relative intensity of peak belonging to rGO increases accordingly and its position does not change obviously. The results suggest the gradual elimination of oxygen-containing groups and the gradual generation of π stacking between rGO sheets [24]. At GO/EDA = 1:50, the peak corresponding to GO can hardly be observed and the peak of rGO remains at 23.25°, corresponding to an interlayer spacing of 3.82 Å which is higher than that of pristine graphite due to the residual unreacted functional groups on rGO sheets and the introduced new functional groups leading to the inhomogeneous crystalline state and poor ordering of rGO sheets [25].

TGA was adopted to check thermal stability of the samples (Fig. 4c). The overall trend of TGA curve for the irradiated GO is the same as the GO. But the total weight loss of the irradiated GO is less than that of GO, indicating the decomposition of labile oxygen functional groups to some degree during γ -ray irradiation. In comparison, all TGA curves of samples with EDA as additive show a slowly downward sloping line which further confirms the elimination of oxygen-containing groups. Meanwhile, the total weight loss of the TGA curves does not differ greatly at GO/EDA ratio \geq 1:10. The weight loss of GA is attributed to two factors: original unreduced functional groups from GO and other new functional groups introduced by EDA-intermediated γ -ray irradiation.

We also studied the evolution of chemical structures using GO/EDA = 1:10 samples irradiated to different doses. The results are shown in Fig. 5 and Tables 3 and 4. The reductive radical species increase with the dose, and so does the reduction degree of GO. It should be mentioned that the GO reduction in an EDA/water solution was accompanied by grafting reaction with the alkyl groups from EDA attached

onto rGO sheets during the irradiation. However, an extremely high dose could destroy the valence bonds of the EDA and make off the alkyl groups from the rGO layer, which results in C/O ratio of rGO turning downwards.

Figure 6a shows the typical FT-IR spectra of GO and the samples irradiated to different doses. At 100 kGy, the characteristic peaks related to oxygen-containing groups like C=O, O-H, and C-O from both carboxyl and alkoxy decrease dramatically, whereas at doses of > 200 kGy, these peaks even disappear entirely.

XRD patterns of the as-prepared GA using at different doses are shown in Fig. 6b. At 100 kGy, only one diffraction peak can be seen at 11.36°. At 200 kGy, a new peak appears at 23.40° due to the partial removal of oxygenous groups and smaller interlayer distance. As the dose further increases, the intensity of peak associated with GO tends to reduce and even disappear, while the intensity of peak belonging to rGO tends to become stronger. Moreover, both peak positions shift to higher degree slightly, reflecting the higher reduction degree and the restoration of crystal lattice structure. Therefore, γ -ray irradiation is an effective method to tune the reduction degree of GO sheets.

As shown in Fig. 6c, thermal stability of GO and the samples increases with the dose due to the reduction of more oxygenous groups on GO sheets. The varying pattern of thermal stability coincides with the variation of C/O ratio from XPS that at 400 kGy the C/O ratio is the highest and the weight loss during heating is the least. A suitable total absorbed dose can be chosen for the reduction and self-assembly of GO sheets.

4 Mechanism

Considering the results of XPS, FT-IR, XRD, and TGA presented above, mechanism of the radiation synthesis of graphene aerogel is supported by chemical structure and thermal stability analysis which provides important

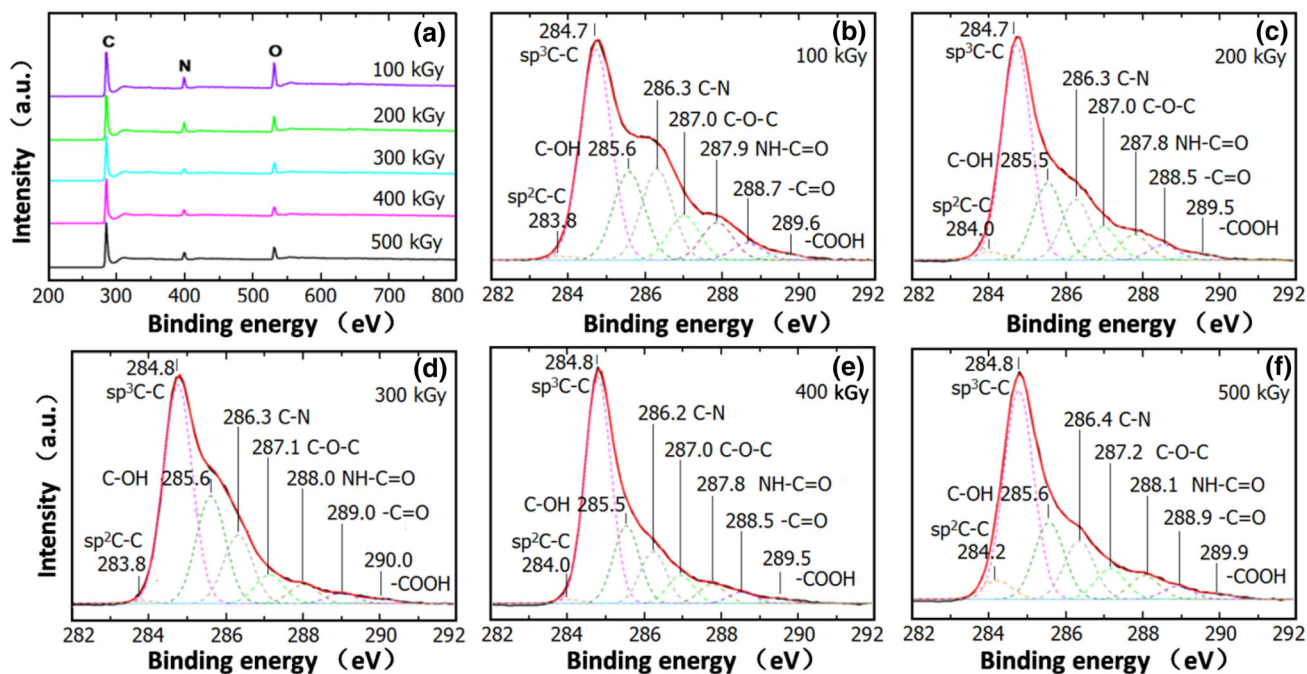


Fig. 5 XPS full-scan spectra of the samples of GO/EDA = 1:10 irradiated to different doses (**a**) and C1s spectra of the samples (**b–f**)

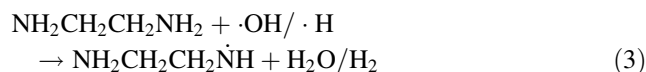
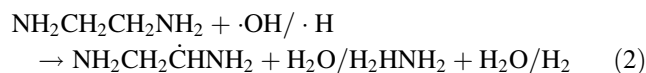
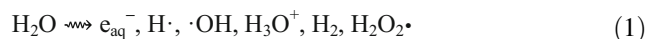
Table 3 Elemental analysis data of samples with different total absorbed dose

Dose (kGy)	Weight percentage			Elemental ratio	
	C	N	O	C/O	C/N
100	67.97	11.30	20.74	4.37	7.02
200	75.42	10.94	14.54	6.83	7.95
300	79.64	6.60	13.76	7.72	14.08
400	79.98	8.87	11.16	9.56	10.52
500	77.72	9.03	13.25	7.82	10.04

information about transformation among different groups during γ -ray irradiation.

According to the radiation chemistry, γ -rays can decompose water molecules into both oxidative and reductive species, as shown in Eq. (1). EDA molecules existing abundantly in the system are speculated to act as radical scavenger and react with oxidative species $\cdot\text{OH}$ and reductive species $\text{H}\cdot$ directly, as presented in Eqs. (2) and (3). And the resulting radicals may take part in the

reactions with functional groups on GO sheets. It is noteworthy to mention here that some EDA molecules may participate in the nucleophilic ring-opening reaction of epoxy groups or the condensation reaction with carboxyl groups directly on the surface of GO regardless of γ -ray irradiation, as demonstrated in Scheme 1b and d, respectively.



In addition, the reductive species like $\text{H}\cdot$ and e_{aq}^- generated in quantities may react with functional groups on GO sheets directly as shown in Scheme 1. The e_{aq}^- may react with carbonyl groups, hence resulting in the formation of hydroxyl in Scheme 1a. And it may also react with

Table 4 XPS-peak-differentiation-imitating information of samples with different total absorbed dose

Dose (kGy)	sp ² C–C	sp ³ C–C	C–OH	C–N	C–O–C	NH–C=O	–C=O	–COOH
100	0.77	42.12	17.74	18.20	8.92	7.52	3.37	1.35
200	1.82	48.70	17.53	13.76	7.56	5.72	3.46	1.45
300	0.55	47.45	23.31	14.88	6.24	4.14	2.27	1.15
400	0.95	53.17	18.36	12.22	6.65	4.58	2.73	1.34
500	4.28	47.94	17.66	13.45	7.04	5.39	2.94	1.30

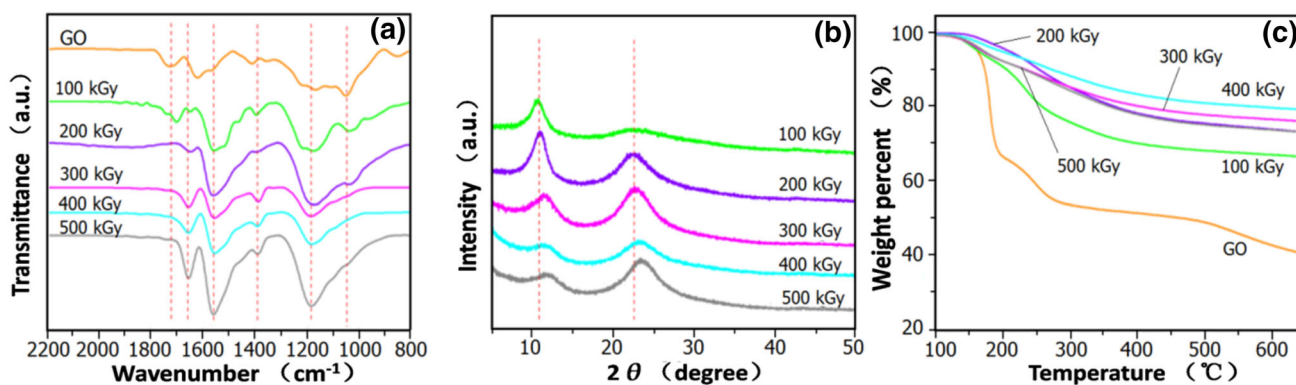
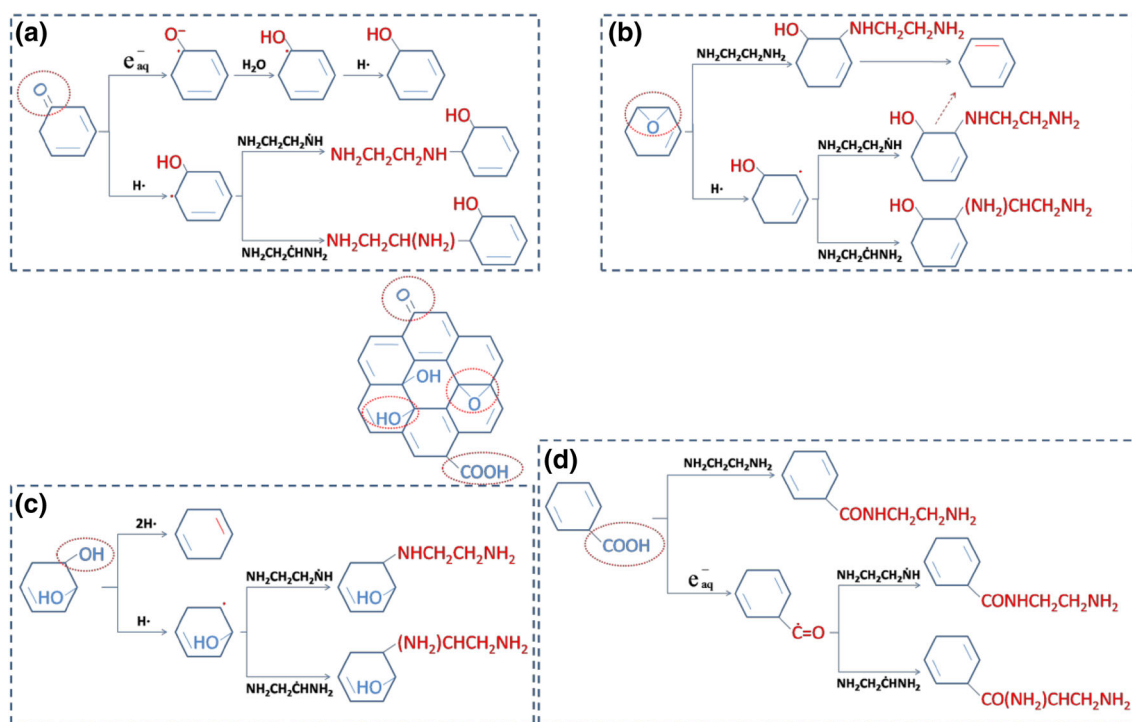


Fig. 6 FT-IR spectra (a), XRD patterns (b), and TGA curves (c) of GO and the samples irradiated to different doses



Scheme 1 Possible reaction mechanism during γ -ray irradiation

carboxyl groups to form ketyl radicals which can recombine with EDA radicals mentioned above in Scheme 1d. Hydrogen radical can add to carboxyl groups in Scheme 1a or split epoxy bridges to form hydroxyl and C–H bonds in Scheme 1b. Also, it may take hydroxyl groups away to form C=C in Scheme 1c. In brief, the reactions between reductive species and oxygen-containing groups may lead to the elimination of oxygen-containing groups, the restoration of conjugated C=C groups, and the introduction of EDA molecules. The reactions in Scheme 1 correspond to the quantitative analysis of functional group composition from XPS C1 s spectra.

5 Conclusion

In summary, the synergy reduction and self-assembly of graphene oxide via γ -ray irradiation in an ethanediamine aqueous solution were studied. Certain amount of EDA and total absorbed dose is preferable for the reduction and formation of graphene aerogel. Without EDA, only irradiation could not result in the self-assembly. C/O ratio of the as-prepared GA increases with the EDA content accordingly and may reach the limit finally. At a low dose, GO sheets can be reduced to some degree and restack together but still cannot complete the self-assembly process

into three-dimensional structure. By increasing the total absorbed dose, the C/O ratio curve shows a peak at 400 kGy. A possible reaction mechanism is proposed based on the analysis results of XPS, FT-IR, XRD, and TGA.

Acknowledgments This study was supported by the National Natural Science Foundation of China (No.11505270) and Shanghai Municipal Commission for Science and Technology (No.15ZR1448300).

References

1. L. Chen, Z. Xu, J. Li, B. Zhou, M. Shan, Y. Li et al., Modifying graphite oxide nanostructures in various media by high-energy irradiation. *RSC Adv* **4**, 1025–1031 (2014). doi:[10.1039/C3RA46203J](https://doi.org/10.1039/C3RA46203J)
2. H. Fujita, M. Izawa, H. Yamazaki, [Gamma]-ray-induced formation of gold sol from chloroauric acid solution. *Nature* **196**, 666–667 (1962). doi:[10.1038/196666a0](https://doi.org/10.1038/196666a0)
3. Y. Bo, J. Cui, Y. Cai, S. Xu, Preparation and characterization of poly(methyl methacrylate) and poly(maleic anhydride-co-diallyl phthalate) grafted carbon black through γ -ray irradiation. *Radiat Phys Chem* **119**, 236–246 (2016). doi:[10.1016/j.radphyschem.2015.11.005](https://doi.org/10.1016/j.radphyschem.2015.11.005)
4. R. Boudens, T. Reid, D. VanMensel, M.R.S. Prakasan, J.J.H. Ciborowski, C.G. Weisener, Bio-physicochemical effects of gamma irradiation treatment for naphthenic acids in oil sands fluid fine tailings. *Sci. Total Environ.* **539**, 114–124 (2016). doi:[10.1016/j.scitotenv.2015.08.125](https://doi.org/10.1016/j.scitotenv.2015.08.125)
5. H. Xu, X. Wang, Y. Zhang, S. Liu, Single-step in situ preparation of polymer-grafted multi-walled carbon nanotube composites under ^{60}Co γ -ray irradiation. *Chem. Mater.* **18**, 2929–2934 (2006). doi:[10.1021/cm052840o](https://doi.org/10.1021/cm052840o)
6. Q. Zhang, Y. Zhang, Z. Gao, H. Ma, S. Wang, J. Peng et al., Facile synthesis of platinum nanoparticle decorated graphene by one-step γ -ray induced reduction for high rate supercapacitors. *J Mater Chem C* **1**, 321–328 (2013). doi:[10.1039/C2TC00078D](https://doi.org/10.1039/C2TC00078D)
7. B. Zhang, L. Li, Z. Wang, S. Xie, Y. Zhang, Y. Shen et al., Radiation induced reduction: an effective and clean route to synthesize functionalized graphene. *J. Mater. Chem.* **22**, 7775–7781 (2012). doi:[10.1039/C2JM16722K](https://doi.org/10.1039/C2JM16722K)
8. Y. Zhang, H. Ma, Q. Zhang, J. Peng, J. Li, M. Zhai et al., Facile synthesis of well-dispersed graphene by [gamma]-ray induced reduction of graphene oxide. *J. Mater. Chem.* **22**, 13064–13069 (2012). doi:[10.1039/C2JM32231E](https://doi.org/10.1039/C2JM32231E)
9. L.F. Dumée, C. Feng, L. He, F.M. Allieux, Z. Yi, W. Gao et al., Tuning the grade of graphene: gamma ray irradiation of free-standing graphene oxide films in gaseous phase. *Appl. Surf. Sci.* **322**, 126–135 (2014). doi:[10.1016/j.apsusc.2014.10.070](https://doi.org/10.1016/j.apsusc.2014.10.070)
10. Z. Wu, Y. Sun, Y. Tan, S. Yang, X. Feng, K. Müllen, Three-dimensional graphene-based macro- and mesoporous frameworks for high-performance electrochemical capacitive energy storage. *J. Am. Chem. Soc.* **134**, 19532–19535 (2012). doi:[10.1021/ja308676h](https://doi.org/10.1021/ja308676h)
11. C. Lu, H. Yang, C. Zhu, X. Chen, G. Chen, A graphene platform for sensing biomolecules. *Angew. Chem. Int. Edit.* **48**, 4785–4787 (2009). doi:[10.1002/anie.200901479](https://doi.org/10.1002/anie.200901479)
12. Z. Wu, S. Yang, Y. Sun, K. Parvez, X. Feng, K. Müllen, 3D nitrogen-doped graphene aerogel-supported Fe_3O_4 nanoparticles as efficient electrocatalysts for the oxygen reduction reaction. *J. Am. Chem. Soc.* **134**, 9082–9085 (2012). doi:[10.1021/ja3030565](https://doi.org/10.1021/ja3030565)
13. H. Cong, X. Ren, P. Wang, S. Yu, Macroscopic multifunctional graphene-based hydrogels and aerogels by a metal ion induced self-assembly process. *ACS Nano* **6**, 2693–2703 (2012). doi:[10.1021/mn300082k](https://doi.org/10.1021/mn300082k)
14. J. Li, J. Li, H. Meng, S. Xie, B. Zhang, L. Li et al., Ultra-light, compressible and fire-resistant graphene aerogel as a highly efficient and recyclable absorbent for organic liquids. *J Mater Chem A* **2**, 2934–2941 (2014). doi:[10.1039/C3TA14725H](https://doi.org/10.1039/C3TA14725H)
15. J. Li, B. Zhang, L. Li, H. Ma, M. Yu, J. Li, γ -ray irradiation effects on graphene oxide in an ethylenediamine aqueous solution. *Radiat Phys Chem* **94**, 80–83 (2014). doi:[10.1016/j.radphyschem.2013.06.029](https://doi.org/10.1016/j.radphyschem.2013.06.029)
16. Y. He, Y. Liu, T. Wu, J. Ma, X. Wang, Q. Gong et al., An environmentally friendly method for the fabrication of reduced graphene oxide foam with a super oil absorption capacity. *J. Hazard. Mater.* **260**, 796–805 (2013). doi:[10.1016/j.jhazmat.2013.06.042](https://doi.org/10.1016/j.jhazmat.2013.06.042)
17. C.-C. Teng, C.-C.M. Ma, C.-H. Lu, S.-Y. Yang, S.-H. Lee, M.-C. Hsiao et al., Thermal conductivity and structure of non-covalent functionalized graphene/epoxy composites. *Carbon* **49**, 5107–5116 (2011). doi:[10.1016/j.carbon.2011.06.095](https://doi.org/10.1016/j.carbon.2011.06.095)
18. S. Park, R.S. Ruoff, Chemical methods for the production of graphenes. *Nat Nano* **4**, 217–224 (2009). doi:[10.1038/nnano.2009.58](https://doi.org/10.1038/nnano.2009.58)
19. S. Park, K.-S. Lee, G. Bozoklu, W. Cai, S.-T. Nguyen, R.S. Ruoff, Graphene oxide papers modified by divalent ions—enhancing mechanical properties via chemical cross-linking. *ACS Nano* **2**, 572–578 (2008). doi:[10.1021/nm700349a](https://doi.org/10.1021/nm700349a)
20. H. Hu, Z. Zhao, W. Wan, Y. Gogotsi, J. Qiu, Ultralight and highly compressible graphene aerogels. *Adv. Mater.* **25**, 2219–2223 (2013). doi:[10.1002/adma.201204530](https://doi.org/10.1002/adma.201204530)
21. J. Li, L. Li, B. Zhang, M. Yu, H. Ma, J. Zhang et al., Synthesis of few-layer reduced graphene oxide for lithium-ion battery electrode materials. *Ind. Eng. Chem. Res.* **53**, 13348–13355 (2014). doi:[10.1021/ie5018282](https://doi.org/10.1021/ie5018282)
22. S.-H. Park, S.-M. Bak, K.-H. Kim, J.-P. Jegal, S.-I. Lee, J. Lee et al., Solid-state microwave irradiation synthesis of high quality graphene nanosheets under hydrogen containing atmosphere. *J. Mater. Chem.* **21**, 680–686 (2011). doi:[10.1039/c0jm01007c](https://doi.org/10.1039/c0jm01007c)
23. S. Yang, L. Zhang, Q. Yang, Z. Zhang, B. Chen, P. Lv et al., Graphene aerogel prepared by thermal evaporation of graphene oxide suspension containing sodium bicarbonate. *J Mater Chem A* **3**, 7950–7958 (2015). doi:[10.1039/C5TA01222H](https://doi.org/10.1039/C5TA01222H)
24. Y. Xu, K. Sheng, C. Li, G. Shi, Self-assembled graphene hydrogel via a one-step hydrothermal process. *ACS Nano* **4**, 4324–4330 (2010). doi:[10.1021/nn101187z](https://doi.org/10.1021/nn101187z)
25. G. Tang, Z.-G. Jiang, X. Li, H.-B. Zhang, A. Dasari, Z.-Z. Yu, Three dimensional graphene aerogels and their electrically conductive composites. *Carbon* **77**, 592–599 (2014). doi:[10.1016/j.carbon.2014.05.063](https://doi.org/10.1016/j.carbon.2014.05.063)